

# Electrostatic discharge in powder-storage silos: Frequency and energy analysis under various conditions

ZHANG Gaoqiang<sup>1</sup>, LI Liangliang<sup>2</sup>, LIANG Cai<sup>1</sup>, MENG He<sup>2</sup>,  
LAN Qi<sup>2</sup>, CHEN Xiaoping<sup>1</sup>, MA Jiliang<sup>1</sup>

(1. School of Energy and Environment, Southeast University, Nanjing 211189, China;  
2. SINOPEC Research Institute of Safety Engineering Co., Ltd., Qingdao 266100, China)

**Abstract:** To explore the electrostatic discharge behavior of charged powders in industrial silos, discharge experiments are conducted based on a full-size industrial silo discharge platform. Electrostatic discharge mode, frequency, and energy are investigated for powders of different polarities. Although the powders have low charge-to-mass ratios (+0.087  $\mu\text{C}/\text{kg}$  for the positively charged powders and  $-0.26 \mu\text{C}/\text{kg}$  for the negatively charged ones), electrostatic discharges occur approximately every 10 s, with the maximum discharge energy being 800 mJ. Powder polarity considerably influences discharge energy. The positive powders exhibit higher discharge energy than the negative ones, although discharge frequency remains similar for both. Effects of powder charge, humidity, and mass flow on discharge frequency and discharge energy are quantitatively analyzed, providing important insights for the improvement of safety in industrial powder handling.

**Key words:** electrostatic discharge; powder; charge-to-mass ratio; discharge frequency; silo

DOI:10.3969/j.issn.1003-7985.2025.01.013

During production, transportation, and storage of powders, static charge accumulates on their surfaces because of frequent contact and separation of particles, as well as interactions with reactor and pipeline walls<sup>[1-3]</sup>. Electrostatics can alter the flow properties in reactors, resulting in particle agglomeration and wall adhesion, which negatively impact product quality<sup>[4-6]</sup>. Charged powders in silos can accumulate static electricity of up to tens of thousands of volts, thereby posing a considerable risk of electrostatic discharge<sup>[7-8]</sup>. The discharges can ignite dust or flammable gases, resulting in fires or explosions that threaten personnel safety and cause substantial economic losses<sup>[9]</sup>. Therefore, study-

ing the electrostatic discharge characteristics in silos is crucial for safe operation of powder handling systems.

Powder charge is influenced by particle properties, operating parameters, and environmental conditions. Lan et al.<sup>[10]</sup> measured the charge-to-mass ratio of polypropylene powders in pneumatic conveying tests and observed values between  $-6$  and  $-7 \mu\text{C}/\text{kg}$ . Tan<sup>[11]</sup> reported that the charge-to-mass ratio in polyolefin silos ranged from  $-10$  to  $+10 \mu\text{C}/\text{kg}$ , with most values between  $-5$  and  $+5 \mu\text{C}/\text{kg}$ . Lei et al.<sup>[12]</sup> investigated the effect of electrostatic fields on interparticle interactions. Cartwright et al.<sup>[13]</sup> observed the bipolar charging of polyethylene powders in silos and noted that particles of different sizes tended to acquire opposite charges during transport. However, the charging and discharge properties of powders with different polarities are still limited. Maurer.<sup>[14]</sup> observed heap surface discharges (cone discharges) in full-scale polyethylene silos and identified them as potential sources of ignition. Glor et al.<sup>[15-17]</sup> investigated electrostatic discharges in silos via monitoring of electric field strength, radio frequency signals, and discharge images. Their results demonstrated that the filling method, silo diameter, and material type affect the discharge laws. Recently, Choi et al.<sup>[18-19]</sup> observed both brush and broad bulk discharges in metal silos by using image intensifiers and investigated the manner in which probe diameter and distance from the powder heap surface influenced the discharge behavior. The discharge energy between the charged powder pile and metal protrusion could reach up to 1000 mJ, which posed considerable risks. Zhou et al.<sup>[20-22]</sup> investigated the discharge patterns during the filling of a silo with different polarity powders and examined the discharging properties of bipolar ionizers. Despite extensive studies on powder charging and discharging behaviors, the discharge frequency and energy-release laws of different polarity powders in silos still remain unclear.

Herein, a full-scale silo discharge platform is used to investigate the electrostatic discharge behavior of different polarity powders. The frequency and energy-release properties of electrostatic discharges are studied through analysis of spatial electric field variations and discharge images. In addition, the effects of powder charge, hu-

Received 2024-09-19, Revised 2024-12-02.

**Biographies:** Zhang Gaoqiang (1995—), male, Ph. D. candidate; Liang Cai (corresponding author), male, doctor, professor, liangc@seu.edu.cn.

**Foundation item:** The National Natural Science Foundation of China (No. 51976039).

**Citation:** ZHANG Gaoqiang, LI Liangliang, LIANG Cai, et al. Electrostatic discharge in powder-storage silos: Frequency and energy analysis under various conditions [J]. Journal of Southeast University (English Edition), 2025, 41 (1): 101-108. DOI: 10.3969/j.issn.1003-7985.2025.01.013.

midity, and filling speed on discharge frequency and energy distribution are investigated.

## 1 Experimental Setup and Methodology

### 1.1 Experimental setup

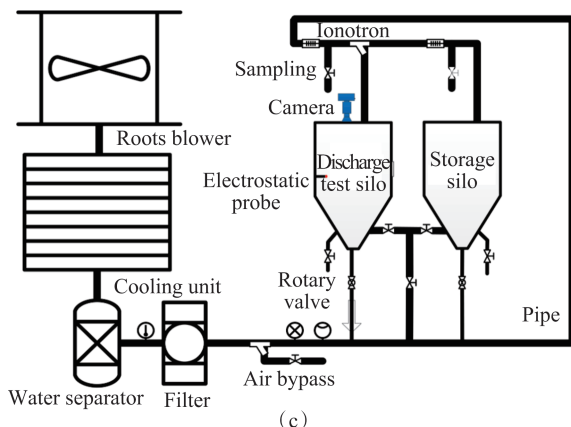
Electrostatic discharge experiments were performed using a full-scale industrial powder conveying system, as shown in Fig. 1. The setup included a Faraday cup and an electrometer to measure the charge-to-mass ratio, as well as an image intensifier and an electric field meter to record discharge properties. The powder discharge system consisted of a gas supply system, a pneumatic conveying system, and an electrostatic detection system.



(a)



(b)



(c)

**Fig. 1** Powder electrostatic discharge test system. (a) Pneumatic conveying system; (b) Powder discharge system; (c) Schematic of powder discharge system

Compressed air from the Roots blower was cooled to ambient temperature, and humidity was adjusted using a water separator and filter. A bypass system was employed to control the airflow. Powder flow into the conveying line was regulated using a rotary valve at the silo outlet. After mixing with a high-velocity air stream, the powder was transported to the discharge silo for a discharge test. A bipolar DC ionotron controller in the pipeline was employed to adjust the powder charge by blowing positive and negative ion winds. Sampling was conducted at the outlet valve before the pipeline entered the silo, and the powder charge-to-mass ratio was obtained via weighing and charge measurement. The discharge silo was equipped with an image intensifier at the top and an electric field probe in the middle so as to continuously record discharge images and electric fields, respectively. During the experiments, the air flow was set to  $26.5 \text{ m}^3/\text{min}$  at a speed of  $39 \text{ m/s}$  and a temperature of  $17.5^\circ\text{C}$ . The conveying pipeline had a diameter of  $0.1 \text{ m}$  and a length of  $35 \text{ m}$ . The discharge silo was  $6 \text{ m}$  high, had a maximum diameter of  $3 \text{ m}$ , and a volume of  $27.9 \text{ m}^3$ . All experimental equipment was made of stainless steel and was well grounded.

### 1.2 Analysis of experimental data

#### 1.2.1 Discharge frequency

As the silo was filled with charged powder, the electric field changed because of powder flow, charge dissipation, and electrostatic discharge, as shown in Figs. 2 and 3. When the positively charged powder entered the silo, rapid accumulation of electrostatic charges increased the electric field strength, as shown in section AB of Fig. 2 (a). When the electric field became sufficiently strong to ionize the air, a large amount of static charge was immediately released, resulting in a rapid decrease in the electric field, as shown in section BC. As charged powder continued to fill the silo, the discharges persisted, and the electric field followed a repeating ABC pattern. For positive-polarity discharges, dot discharges exhibited low discharge intensity, resulting in minimal changes in the electric field. Linear discharges originated from dot discharges, with longer discharge paths and more charge release, hence resulting in greater changes in the electric field. Dendritic discharges were observed to be extended modes of linear discharges, which have longer discharge paths and can release more charge, resulting in notable fluctuations in the electric field. Fluctuations in the electric field were extracted from electric field variations, as shown in Fig. 2 (b). The electric field data and discharge images indicated that different discharge patterns caused different variations in electric field fluctuation. The regular and anomaly areas in this study were defined: strong discharges caused notable fluctuations, while weaker dis-

charges or particle flows caused slight changes. We focus on the strong electrostatic discharges ( $\Delta E > 5$  kV/m) because they are more dangerous. Weak discharges, characterized by minimal variations in field strength, as well as fluctuations during the filling process caused by factors such as instability in filling rate and randomness in charging parameters, are excluded from consideration. Powder polarity affects the fluctuation direction of electric field strength, as shown in Fig. 3. When the silo was filled with negatively charged powders, the discharges were typically brush and broad bulk ones. The brush discharges are continuously generated near the silo wall, and they could ignite combustible gases with an equivalent ignition energy of less than 3.6 mJ. The ring shape of brush discharges was clearly captured, as shown in Fig. 3. These discharges appeared as small, concentrated, and often linear patterns, resembling the bristles of a brush. During brush discharges, the release of charge is less and the discharge energy tends to be lower in comparison with other types of discharges, resulting in minimal fluctuations in electric field strength. Broad

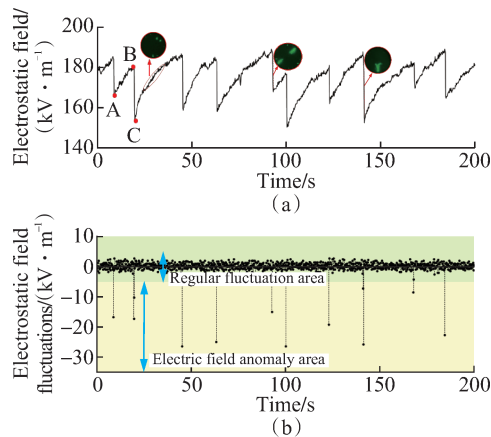


**Fig. 2** Spatial electric field variation with positive-polarity powder filling. (a) Original electric field; (b) Fluctuations in electric field strength

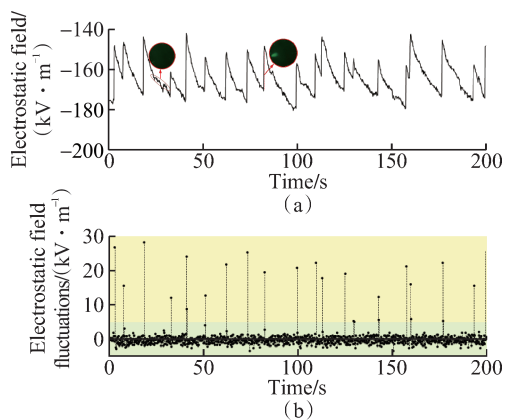


**Fig. 3** Spatial electric field variation with negative-polarity powder filling. (a) Original electric field; (b) Fluctuations in electric field strength

bulk discharges often occurred at the heap surface, where the brush discharges could not reach, and they could easily ignite gases or dust with an equivalent ignition energy of more than 10 mJ. The broad bulk discharge exhibited a feather-like shape, and the larger discharge area meant that more molecules were ionized and more charges were emitted, which considerably changed the electric field. Herein, we investigated the effect of charge-to-mass ratio and other experimental conditions on electrostatic discharge characteristics. Charging type of particles could notably influence discharge behavior. In particular, positively charged ions may interact differently with particles compared with negatively charged electrons. Results of experiments demonstrated that discharge patterns for different polarity powders were unaffected by ionic wind. However, further research is needed to determine whether the minimum charge-to-mass ratio required to induce discharge is influenced by the charging type of powder. To minimize potential errors, the ionized wind was solely used to charge only positively polarized powders.

### 1.2.2 Discharge energy

The electric field inside the silo was simulated on the basis of experimental data so as to determine the relationship between electrostatic field charge and static charge released by powder. Electrostatic discharge energy ( $w_e$ ) was calculated using charge transfer ( $\Delta Q$ )<sup>[23]</sup>. An electrostatic field model of the charged-powder silo was established using COMSOL Multiphysics. The silo model included charged powder and air, as shown in Fig. 4. The model and experimental silo had identical dimensions, with a powder dielectric constant of 3.2. The minimum grid size was set to 0.1 mm, and the maximum growth rate was set to 1.2. The model has been widely used to calculate electrostatic field distributions in silos<sup>[24]</sup>.

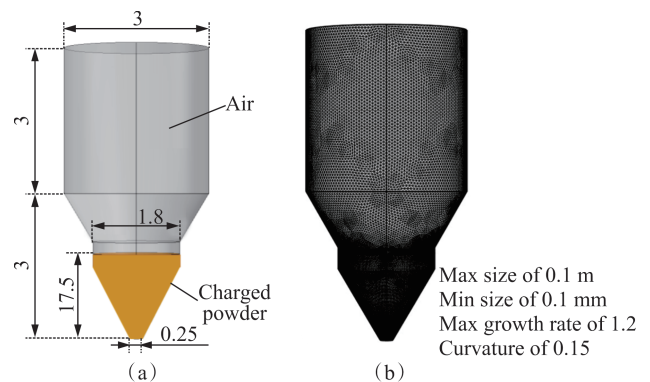


**Fig. 4** Schematic of discharge silo mode. (a) Silo model (unit: m); (b) Grid

The distribution of electrostatic potential in the powder and gas space was calculated using Poisson's and Laplace's equations, respectively.

$$\nabla^2 \phi = \begin{cases} -\rho/(\varepsilon_r \varepsilon_0) & \text{Powder space} \\ 0 & \text{Gas space} \end{cases} \quad (1)$$

where  $\phi$  denotes the electric potential in the silo;  $\varepsilon_0$  is the permittivity of vacuum (8.854 pF/m);  $\varepsilon_r$  is the relative permittivity of the material. The electric field strength  $E$  (V/m) in the silo is defined as the gradient of the potential.

$$E = -\nabla\phi \quad (2)$$

With the metal silo being well grounded, the boundary conditions are

$$\begin{cases} \phi = 0, z = 0 \\ \phi = 0, r = D/2 \\ \phi = 0, z = H \end{cases} \quad (3)$$

where  $H$  denotes the height of the silo, and  $D$  is the diameter of the powder heap. For the powder-gas interface, it is assumed that there exists no surface charge on the powder heap surface. Therefore,

$$\phi_{\text{gas}} = \phi_{\text{powder}} \quad (4)$$

$$\frac{\partial \phi_{\text{gas}}}{\partial z} = \frac{\varepsilon_r \partial \phi_{\text{powder}}}{\partial z} \quad (5)$$

$$\frac{\partial \phi_{\text{gas}}}{\partial r} = \frac{\partial \phi_{\text{powder}}}{\partial r} \quad (6)$$

where  $\phi_{\text{gas}}$  and  $\phi_{\text{powder}}$  denote electric potentials in the gas and powder spaces, respectively.

The relationship between electric field changes at the measuring point and the released charge of charged powder is described in Eq. (7) on the basis of the simulation results. The electric field increases linearly with the filled powder charge. The powder charge increased from 6 to 43  $\mu\text{C}$  when the electric field was changed from 10 to 80 kV/m. Combined with empirical equations for discharge energy derived from the experiments in Ref. [23], the relationship between electric field fluctuations and discharge energy is outlined in Eq. (8). When electric field fluctuations increased from 10 to 80 kV/m, the discharge energy increased from 100 to 900 mJ. This study examined the electrostatic discharge energy using the fitting formula in Eq. (8), which relates electric field changes to discharge energy in our experiments.

$$\Delta Q = 0.523\Delta E \quad (7)$$

$$w_e = 9.188\Delta E^2 + 0.027\Delta E - 25.93 \quad (8)$$

where  $\Delta E$  represents the change in electric field strength at the measurement point.

## 2 Results and Discussion

### 2.1 Effect of powder charge on electrostatic discharge

The polarity and powder charge directly determined the electric field distribution and strength in the silo, affecting the discharge pattern, frequency, and intensity.

At the same filling speed of 1.8 kg/s and humidity of 45%, the electrostatic discharge frequency  $F_e$  and maximum discharge energy  $M_e$  of powders with different charge-to-mass ratios and polarities are presented in Table 1. The discharge frequency and maximum discharge energy rose with the increase in the charge-to-mass ratio  $M$  of the powders. For positively charged powders, with their charge-to-mass ratio increasing from +0.087 to +0.273  $\mu\text{C}/\text{kg}$ , the average discharge period decreased from 21.2 to 13.9 s, and the maximum discharge energy increased from 237 to 434 mJ. For negatively charged powders, with the charge-to-mass ratio increasing from -0.26 to -0.452  $\mu\text{C}/\text{kg}$ , the average discharge period decreased from 12.5 to 5.3 s, and the maximum discharge energy increased from 226 to 541 mJ. A higher powder charge notably increased the risk of electrostatic discharge. At the same charge, positively and negatively charged powders exhibited similar discharge frequencies, but the maximum discharge energy of positively charged powders was twice that of negatively charged ones. Fig. 5 shows the energy probability distribution of different polarity powders. The results indicated that increasing the charge-to-mass ratio  $M$  resulted in higher discharge energy and a greater probability of high-energy discharge, irrespective of powder polarity. Figs. 5(b) and (c) show the differences in the discharge energy distribution of different polarity powders with the same powder charge. Positively charged powders released more discharge energy, with a 41% probability of exceeding 300 mJ, while only 6% of nega-

**Table 1** Discharge frequency and energy of powders with different charge-to-mass ratios

$M/(\mu\text{C}\cdot\text{kg}^{-1})$	Period/s	$F_e/s^{-1}$	$M_e/\text{mJ}$
+0.087	21.18	0.047	237
+0.273	13.90	0.072	434
-0.260	12.50	0.080	226
-0.452	5.33	0.188	541

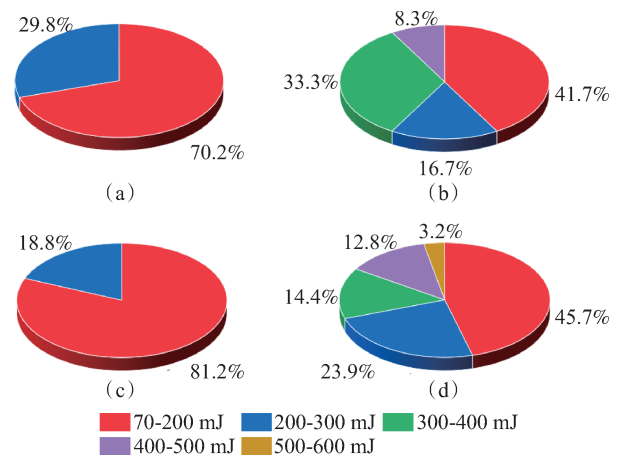


**Fig. 5** Discharge energy distribution of powders with different charge-to-mass ratios. (a)  $M=+0.087 \mu\text{C}/\text{kg}$ ; (b)  $M=+0.273 \mu\text{C}/\text{kg}$ ; (c)  $M=-0.260 \mu\text{C}/\text{kg}$ ; (d)  $M=-0.452 \mu\text{C}/\text{kg}$

tively charged powders surpassed this threshold. In summary, positively charged powders had considerably higher electrostatic ignition probability than negatively charged ones.

## 2.2 Effect of humidity on electrostatic discharge

Humidity considerably influences the breakdown threshold of the air and plasma development and also affects the frequency and energy of electrostatic discharges. Charge-to-mass ratios and filling speeds of the powders were kept constant to investigate the effect of humidity on electrostatic discharge, and the results are presented in Table 2. Humidity  $H_u$  exerted different effects on discharge properties depending on powder polarity. For positively charged powders, increased humidity notably increased both the discharge frequency and maximum discharge energy. When  $H_u$  was increased from 45% to 75%, the average discharge period decreased from 14 to 5.8 s, and the maximum discharge energy increased from 434 to 794 mJ. Conversely, for negatively charged powders, the maximum discharge energy was enhanced with increasing humidity (from 541 to 804 mJ), but the discharge periods remained unchanged. A humid environment facilitated movement and release of charges, and the energy of electrostatic discharge may have increased because of higher conductivity. Fig. 6 shows the energy probability distribution of electrostatic discharges at different humidities. The results demonstrated that higher humidity resulted in greater energy release in discharges of different polarity powders. For positive discharges, the discharge energy above 500 mJ increased from 0% to 23.1% when  $H_u$  was increased from 45% to 75%. In comparison, the proportion of negative discharges increased from 3.2% to 16.4%. Conductivity and charge distribution of positively and negatively charged powders could vary under humidity conditions. With increasing humidity, the water molecules could affect the charge distribution on the surface of the powders, altering their discharge behaviors. Positively charged powders may have been more prone to water adsorption, enhancing their discharge performance, while negatively charged powders may have experienced limited charge release under humid conditions. In conclusion, higher humidity increased discharge energy, notably raising the frequency for positively charged powders but exerting a weak effect on negatively charged powders.

**Table 2** Discharge frequency and energy of powders at different humidities

$H_u/\%$	$M/(\mu\text{C}\cdot\text{kg}^{-1})$	Period/s	$F_c/s^{-1}$	$M_c/\text{mJ}$
45	+0.273	13.90	0.072	434
75	+0.315	5.78	0.173	794
45	-0.452	5.33	0.188	541
75	-0.456	5.88	0.170	804

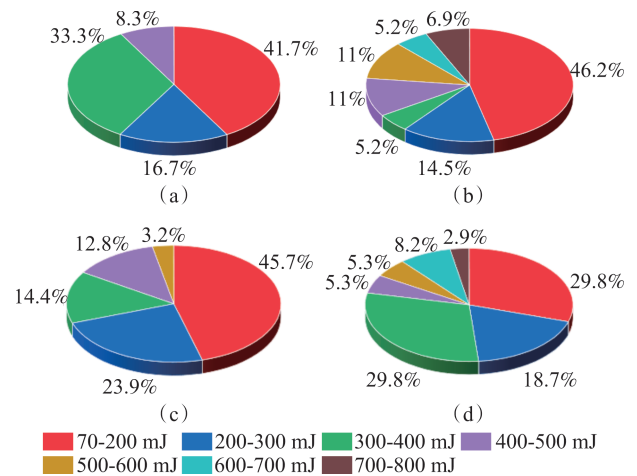


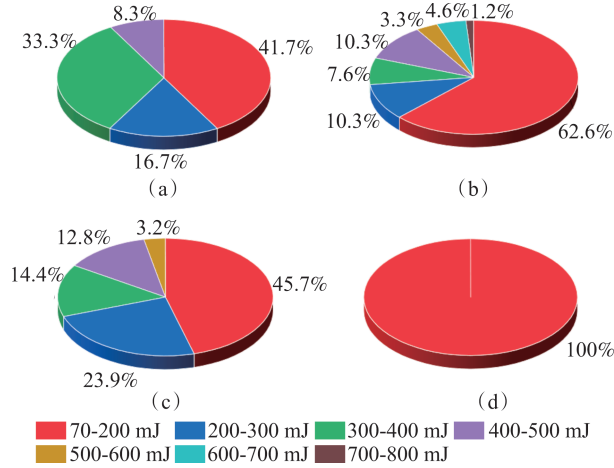
**Fig. 6** Discharge energy distribution of powder at different humidities. (a)  $H_u=(45\pm 10)\%$ ,  $q>0$ ; (b)  $H_u=(75\pm 10)\%$ ,  $q>0$ ; (c)  $H_u=(45\pm 10)\%$ ,  $q<0$ ; (d)  $H_u=(75\pm 10)\%$ ,  $q<0$

## 2.3 Effect of filling speed on electrostatic discharge

The discharging and discharge characteristics of different polarity powders in the silo were observed to be influenced by the filling speed. Under the same humidity conditions, both the frequency of electrostatic discharge and the maximum energy of electrostatic discharge at different powder filling speeds are presented in Table 3. Effects of filling speed on discharge frequency and energy varied with powder polarity. For positively charged powders, a higher filling speed notably increased discharge frequency and maximum energy. As the filling speed was increased from 1.82 to 3.40 kg/s, the charge-to-mass ratio rose from +0.273 to +0.456  $\mu\text{C}/\text{kg}$ ; the average discharge period shortened from 21 to 3 s; and the maximum discharge energy increased from 434 to 726 mJ. For negatively charged powders, a higher filling speed shortened the discharge period but notably reduced the maximum energy. This was attributed to the difference in discharge patterns between different polarity powders. For negatively charged powders, a higher filling speed facilitated brush discharges and inhibited broad bulk discharges. However, a higher filling speed could help point discharges evolve into longer-path and higher-energy discharge forms in positive powder silos. Fig. 7 shows the probability distribution of discharge energy at different filling speeds. For positively charged powders, as the filling speed  $S_p$  increased, the maximum discharge energy increased, but the discharge proportion with less than 200 mJ energy also rose. Conversely, for negatively charged powders, as the filling speed increased, the maximum discharge energy decreased, with all discharge energies less than 200 mJ. The results indicated that a higher filling speed increased the risk in the case of positively charged powders. In contrast, the risk decreased in the case of negatively charged powders under the same conditions.

**Table 3** Discharge frequency and energy of powders at different mass flow rates

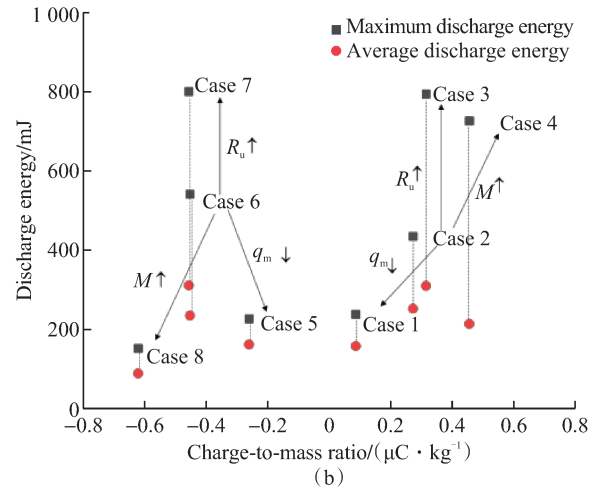
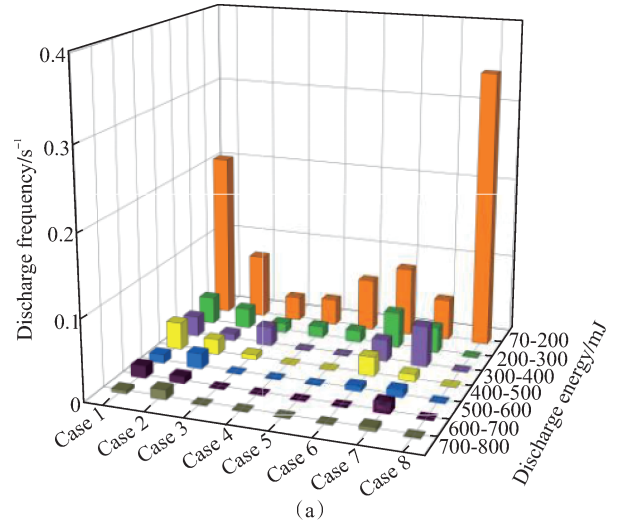
$S_p/(\text{kg}\cdot\text{s}^{-1})$	$M/(\mu\text{C}\cdot\text{kg}^{-1})$	Period/s	$F_d/\text{s}^{-1}$	$M_d/\text{mJ}$
1.82	+0.273	21.180	0.047	434
3.40	+0.456	3.050	0.328	726
1.82	-0.452	5.330	0.188	541
3.40	-0.621	2.920	0.343	151

**Fig. 7** Discharge energy distribution of powder at different filling speeds. (a)  $S_p=1.82 \text{ kg/s}, q>0$ ; (b)  $S_p=3.4 \text{ kg/s}, q>0$ ; (c)  $S_p=1.82 \text{ kg/s}, q<0$ ; (d)  $S_p=3.4 \text{ kg/s}, q<0$ 

#### 2.4 Discharge correlation analysis under different conditions

The relationship among electrostatic discharge frequency, discharge energy, and charge-to-mass ratio under varying conditions of charge, humidity, and filling speed is shown in Fig. 8. Fig. 8(a) shows the frequency distribution of discharge under different conditions. Cases 1 to 4 and Cases 5 to 8 represent experiments for positively and negatively charged powders, respectively, under different discharge conditions (Table 4). For positively charged powders, both the discharge frequency and energy increased at higher charge-to-mass ratios (Cases 1 and 2), humidity (Cases 2 and 3), and filling speeds (Cases 2 to 4). For negatively charged powders, a higher charge-to-mass ratio (Cases 5 and 6) and humidity (Cases 6 and 7) notably increased the discharge frequency and energy, while a higher filling speed (Cases 6 to 8) reduced the maximum discharge energy. Fig. 8(b) shows the energy variation of electrostatic discharges under different discharge conditions. The maximum and average energies of discharges from different polarity powders increased at higher charge-to-mass ratios and humidity. In particular, an increase in humidity considerably increased the maximum discharge energy. For positively charged powders, an increase in filling speed increased the maximum discharge energy but reduced the average discharge energy. For negatively charged powders, an increase in filling speed decreased both the maximum

and average discharge energies. In conclusion, discharge frequency and energy rose with the charge-to-mass ratio. Higher humidity considerably increased discharge energy, but discharge frequency greatly varied with different polarity powders. An increase in filling speed facilitated longer discharge paths in positively charged powders but suppressed broad bulk discharges in negatively charged ones.

**Fig. 8** Distributions of discharge frequency and discharge energy under different discharge conditions. (a) Discharge frequency; (b) Discharge energy**Table 4** Experiments under different discharge conditions

Case No.	1	2	3	4	5	6	7	8
$S_p/(\text{kg}\cdot\text{s}^{-1})$	1.82	1.82	1.82	3.40	1.82	1.82	1.82	3.40
$M/(\mu\text{C}\cdot\text{kg}^{-1})$	0.087	0.273	0.315	0.456	-0.260	-0.452	-0.456	-0.621
$H_u/\%$	45	45	75	45	45	45	75	45

### 3 Conclusions

(1) Electrostatic discharge frequently occurred in industrial silos when the charge-to-mass ratio of different polarity powders was only +0.087 and -0.26  $\mu\text{C}/\text{kg}$ .

For positively charged powders, the average discharge period was 21 s with a maximum energy release of 237 mJ, while for negatively charged powders, the average discharge period was 5.8 s with a maximum energy release of 400 mJ.

(2) With the increase in the charge-to-mass ratio, both the discharge frequency and maximum energy considerably increase for different polarity powders. Although discharge frequencies were similar both for positively and negatively charged powders at the same charge-to-mass ratio, discharge energy was consistently higher for the former ones.

(3) For the same powder charge and filling speed, discharge energy notably increased with humidity. When humidity was increased from 45% to 75%, the maximum discharge energy of positively charged powders increased from 434 to 794 mJ, while that of negatively charged ones increased from 541 to 804 mJ. Under high-humidity conditions, the discharge frequency of positively charged powders sharply increased, but that of negatively charged powders slightly increased.

(4) For positively charged powders, increased filling speed considerably increased discharge frequency and energy. In addition, with an increase in filling speed from 1.82 to 3.4 kg/s, discharge frequency increased from 0.071 to 0.328, and maximum discharge energy increased from 434 to 726 mJ. In contrast, for negatively charged powders, discharge energy notably decreased, but discharge frequency increased.

## References

- [1] HU J W. Study on charging characteristics and electrostatic effect of moving particles[D]. Nanjing: Southeast University, 2021. (in Chinese)
- [2] ZHOU Q. Research on the characteristics of electrostatic distribution of charged powder in silo and regulation method [D]. Nanjing: Southeast University, 2022. (in Chinese)
- [3] WU J T, QIU L, JIAO Y, et al. Identification and analysis of mixing-induced homogeneity in reclaimed asphalt pavement materials[J]. *Journal of Southeast University (English Edition)*, 2024, 40(2): 193-202.
- [4] FOTOVAT F, BI X T, GRACE J R. A perspective on electrostatics in gas-solid fluidized beds: Challenges and future research needs [J]. *Powder Technology*, 2018, 329: 65-75.
- [5] WANG Z, PANG L, SHAO Y J, et al. Experimental study on fluidized attrition characteristics and mechanism of quartz sand particles[J]. *Journal of Southeast University (Natural Science Edition)*, 2024, 54(2): 503-512. (in Chinese)
- [6] KONG L Y, ZENG Q L, ZHANG Z Q, et al. Antiskid decay prediction of asphalt mixtures based on aggregate mechanical properties and gradation fractals[J]. *Journal of Southeast University (English Edition)*, 2024, 40(1): 58-67.
- [7] GLOR M. Ignition hazard due to static electricity in particulate processes[J]. *Powder Technology*, 2003, 135: 223-233.
- [8] FU F F, XU C L, WANG S M, et al. Kinematic characterization of dense-phase pulverized coal particles for pneumatic conveying based on arrayed electrostatic sensors[J]. *Journal of Southeast University (Natural Science Edition)*, 2013, 43(3): 536-541. (in Chinese)
- [9] EGAN S. Learning lessons from five electrostatic incidents[J]. *Journal of Electrostatics*, 2017, 88: 183-189.
- [10] LAN Q, LI L L, LIANG C, et al. Experimental study on the effect of vibration charging characteristics of spherical polypropylene particles[J]. *Acta Petrolei Sinica*, 2022, 38(4): 903-909.
- [11] TAN F G, SONG W, GONG H, et al. Research on the static electricity of petrochemical powder pneumatic conveying and prevention of dust electrostatic explosion[J]. *Journal of Physics: Conference Series*, 2013, 418: 012026.
- [12] LEI B J, YIN Y G, FAN F S. Mechanism of electrostatic field on interface and particle interaction between salt solution and air[J]. *Journal of Southeast University (Natural Science Edition)*, 2024, 54(2): 487-494. (in Chinese)
- [13] CARTWRIGHT P, SINGH S, BAILEY A G, et al. Electrostatic charging characteristics of polyethylene powder during pneumatic conveying[J]. *IEEE Transactions on Industry Applications*, 1985, IA-21(2): 541-546.
- [14] MAURER B. Discharges resulting from electrostatic charging in large storage silos[J]. *Chemical Engineering & Technology*, 1979, 51: 98-103.
- [15] GLOR M. Hazards due to electrostatic charging of powders [J]. *Journal of Electrostatics*, 1985, 16(2/3): 175-191. DOI: 10.1016/0304-3886(85)90041-5.
- [16] GLOR M, LÜTTGENS G, MAURER B, et al. Discharges from bulked polymeric granules during the filling of silos—characterization by measurements and influencing factors [J]. *Journal of Electrostatics*, 1989, 23: 35-43.
- [17] GLOR M, MAURER B. Ignition tests with discharges from bulked polymeric granules in silos (cone discharges) [J]. *Journal of Electrostatics*, 1993, 30: 123-133.
- [18] CHOI K, ENDO Y, SUZUKI T. Experimental study on electrostatic charges and discharges inside storage silo during loading of polypropylene powders [J]. *Powder Technology*, 2018, 331: 68-73.
- [19] CHOI K, OSADA Y, ENDO Y, et al. Experimental study on the effect of metal protrusions inside silos on electrostatic discharges [J]. *Powder Technology*, 2020, 366: 661-666.
- [20] ZHOU Q, LI L L, BI X T, et al. Electrostatic elimination of charged particles by DC-type bipolar electrostatic eliminator [J]. *Powder Technology*, 2022, 408: 117774.
- [21] ZHANG G Q, LI L L, ZHOU Q, et al. Electrostatic discharge pattern and energy probability distribution of dif-

- ferent polarity powders in industrial silo [J]. Chemical Engineering Research and Design, 2023, 192: 91-101.
- [22] ZHANG G Q, WANG Q, LIANG C, et al. Electrostatic discharge mechanisms and dynamic characteristics of different polarity powders in the Silo [J]. Powder Technology, 2024, 441: 119819.
- [23] GLOR M, MAURER B, ROGERS R. Ignition tests during filling of different types of flexible intermediate bulk containers (FIBCs) with polymers [J]. Journal of Physics: Conference Series, 1995, 143: 121-124.
- [24] ZHOU Q, HU J W, LIANG C, et al. Study on electric field distribution in cylindrical metal silo containing charged polyethylene powder [J]. Powder Technology, 2019, 353: 145-155.

## 不同条件下料仓荷电粉体静电放电频率及能量释放特性研究

张高强<sup>1</sup>, 李亮亮<sup>2</sup>, 梁财<sup>1</sup>, 孟鹤<sup>2</sup>, 兰琦<sup>2</sup>, 陈晓平<sup>1</sup>, 马吉亮<sup>1</sup>

(1. 东南大学能源与环境学院, 南京 211189; 2. 中石化安全工程研究院, 青岛 266100)

**摘要:** 为探究工业料仓粉体静电放电特性, 基于全尺寸工业料仓粉体输送平台进行荷电粉体放电试验研究, 获得了料仓粉体静电放电频率及能量释放特性。结果表明, 料仓填充正/负极性粉体时, 荷质比分别低至 +0.087 和 -0.26  $\mu\text{C}/\text{kg}$ , 料仓中仍然频繁发生静电放电, 且平均放电周期仅约为 10 s, 最大放电能量达到 800 mJ。粉体荷电极性对静电放电能量分布影响显著, 在相同的荷质比下, 料仓填充正极性粉体时平均放电能量显著高于负极性粉体, 但二者放电频率相差不大。定量研究了不同粉体荷质比、空气湿度和粉体质量流量对粉体放电频率以及能量释放的影响, 获得了 3 种条件变化下粉体放电的最大释放能量、平均释放能量以及能量分布特性。

**关键词:** 静电放电; 粉体; 荷质比; 放电频率; 料仓

**中图分类号:** TB126